

# The 3p photoabsorption spectra of $\text{Mn}^{2+}$ and $\text{Mn}^{3+}$

D. Kilbane,<sup>1</sup> R. Mayo,<sup>2</sup> C. Banahan,<sup>1</sup> P. van Kampen,<sup>1</sup> J.-P. Mosnier,<sup>1</sup> E. T. Kennedy,<sup>1</sup> and J. T. Costello<sup>1</sup>

<sup>1</sup>*NCPST and The School of Physical Sciences, Dublin City University, Ireland*

<sup>2</sup>*Univ Complutense Madrid, Fac Ciencias Fis, Dpto Fis Atom Mol and Nucl, Madrid, E-28040 Spain*

Time resolved EUV photoabsorption spectra of a manganese plasma have been recorded using the dual laser plasma technique. The 43 - 73 eV photon energy range is dominated by the 3p-3d giant resonance and to a lesser extent the 3p-4s resonances in both  $\text{Mn}^{2+}$  and  $\text{Mn}^{3+}$ , recorded at an interplasma time delay of 80 ns and 30 ns respectively. These experimentally observed resonances are well reproduced by synthetic spectra calculated using the Hartree-Fock method. The synthetic spectra allow for absorption from excited states of the  $\text{Mn}^{2+}$  and  $\text{Mn}^{3+}$  ions.

PACS numbers: 31.10.+z,32.30.Jc,32.70.Cs,32.80.Dz,32.80.Fb,32.80.Hd

## I. INTRODUCTION

Atomic photoionization of free iron-group elements in the region of inner shell 3p-3d giant resonances has been the focus of a great deal of interest in the past decade. EUV photoabsorption and photoion spectra of ions of chromium (Costello et al [1], McGuinness et al [2, 3], West et al [4]), manganese (Cooper et al [5], Costello et al [1], Kjeldsen et al [6]) and iron (Kjeldsen [7]) and theoretical studies by Dolmatov [8–12] and Donnelly [13–16] gave rise to significant debate. A recent photoabsorption experiment by Kilbane et al [17] confirmed Dolmatov's predictions [9], that between  $\text{Mn}^+$  and  $\text{Mn}^{2+}$ , not only do the 3p-4s resonances swap over to the high energy side of the giant 3p-3d resonance but also that this reordering has significant effects on the resonance profiles.

In addition to the spectroscopic knowledge of the atomic structure gained by such studies, manganese and its ions are of particular importance due to the significant roles they play in numerous magnetic materials. Recently there have been a number of studies on the connection between the electronic structure and magnetic properties of compounds containing transition-metals, e.g. a perovskite manganite such as  $\text{LaMnO}_3$  [18] and mixed valence manganites such as  $A_{0.7}^{3+}B_{0.3}^{2+}(\text{MnO}_3)$  [19]. The magnetic properties of such compounds depend greatly on the degree of ionization of the manganese ions present. The starting point for a theoretical description of these manganites, such as in the *ab initio* crystal Hartree-Fock approximation [20], is a knowledge of the electronic structure of the free  $\text{Mn}^{3+}$  ion.

In this paper we investigate the spatial and temporal evolution of a manganese plasma with a view to isolating and studying EUV photoabsorption by  $\text{Mn}^{2+}$  and  $\text{Mn}^{3+}$  ions. The paper is organized as follows. The experiment is described in section II. In section III the measured spectra are presented and compared with the synthetic spectra produced using configuration interaction (CI) Hartree-Fock calculations and accounting for contributions to the spectra from metastable states of the  $\text{Mn}^{2+}$  and  $\text{Mn}^{3+}$  ions. Conclusions are reached in section IV.

## II. EXPERIMENT

The dual laser plasma (DLP) technique [21] was used to record the manganese spectra in this experiment. A Nd:YAG laser (0.7 J in 15 ns) was used to create the absorbing (Mn) plasma, while a second Nd:YAG laser (0.65 J in 15 ns) tightly focussed onto a tungsten target was used to create the backlighting EUV continuum plasma. Optimization of absorption due to a particular ionic species was achieved by variation of the time delay ( $\delta\tau$ ) between the generation of the absorbing and continuum emitting plasmas and of the position of the absorbing plasma with respect to the optic axis ( $\delta l$ ). Spectra were recorded photoelectrically with a McPherson 2.2 m grazing incidence vacuum spectrograph fitted with an image intensified microchannel plate assembly coupled to a photodiode array detector [21]. The spectra were calibrated against known emission lines of aluminium and the system has an instrumental resolution of better than 0.07 eV in the photon energy range used.

## III. RESULTS AND DISCUSSIONS

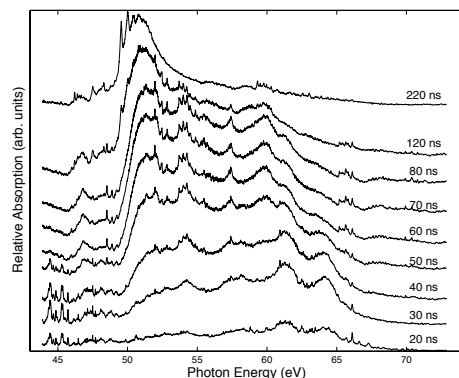


FIG. 1: The temporal evolution of the photoabsorption spectrum of a manganese plasma at a position of  $\delta l = 1$  mm

The temporal evolution of the manganese plasma is shown in Fig. 1, for a range of inter plasma time delays

from 20 – 200 ns, at a position of  $\delta l = 1$  mm from the optic axis. At long time delays (220 ns) photoabsorption due to  $\text{Mn}^+$  (Cooper et al [5] and Costello et al [1]) is clearly evident where the three features on the low energy side of the broad 3p-3d giant resonance are known to be 3p-4s resonances. At an intermediate time delay of 80 ns, these low energy resonances have disappeared and photoabsorption due to  $\text{Mn}^{2+}$  is apparent with discrete structure due to 3p-4s resonances appearing on the high energy side of the giant 3p-3d resonance as reported in [17]. At a shorter time delay of 30 ns photoabsorption is predominantly due to  $\text{Mn}^{3+}$  as is indicated by the presence of discrete structure belonging to this ion at  $\sim 45$  eV.

### A. Synthetic Spectra for 3p excitations of $\text{Mn}^{2+}$

As was alluded to in [17], in recording the photoabsorption spectrum of doubly ionized manganese, it was not possible to eliminate metastable ions from the plasma sample because they lie within the excitation temperature of the ground state ion. We account for these metastable contributions by superimposing calculated cross sections for several individual low-lying terms weighted according to a Boltzmann distribution for several plasma temperatures [2, 3]. A multitude of low lying states are positioned above the  $3d^5$   ${}^6S_{5/2}$  ground state and extend beyond the next lowest configuration state,  $3d^44s$   ${}^6D_{1/2}$ , which lies at 7.744 eV [22]. Configuration-interaction calculations were performed using the HXR (Hartree plus exchange plus relativistic corrections) mode of the Cowan code [23] for the basis set defined in Table I. In order to compensate for the effect of missing configurations, the Slater parameters  $F^k$ ,  $G^k$  and the configuration interaction parameter  $R^k$  were fixed at 0.85 of the *ab initio* values while the spin-orbit parameter was left unchanged.

TABLE I: Configurations included in the CI calculation for the 3p-excitations of  $\text{Mn}^{2+}$

Ground states	Discrete states	Continuum channels	
$3p^63d^5$	$3p^53d^6$ <sup>a</sup>	$3p^63d^44p$	$3p^63d^4 + \epsilon l$
$3p^63d^44s$	$3p^53d^54s$ <sup>a</sup>	$3p^63d^45p$	$3p^63d^34s + \epsilon' l$
	$3p^53d^55s$ <sup>a</sup>	$3p^63d^44f$	
	$3p^53d^56s$ <sup>a</sup>	$3p^63d^45f$	
	$3p^53d^54d$ <sup>a</sup>	$3p^53d^44s^2$ <sup>a</sup>	

<sup>a</sup> denotes levels from which autoionization was energetically possible.

Autoionization calculations were performed to determine the decay widths of the excited  $3p^{-1}$  states. The decay schemes were restricted to the excited states labelled 'a' coupled to both continuum channels (see table I). Synthetic spectra were constructed by assuming a Lorentzian line profile,  $\sigma(E) = 109.7 f_k \Gamma_k / 2\pi [(E_k - E)^2 +$

$\Gamma_k^2/4]$ , where  $E_k$  and  $\Gamma_k$  are the energy and autoionization decay width of the transition in eV,  $f_k$  is the oscillator strength and  $\sigma$  is obtained in Mb. In Figure 2 the calculated cross section for each of the following transitions is presented:  $3p^63d^5 \rightarrow 3p^53d^6$ ,  $3p^53d^54s$ ,  $3p^53d^55s$ ,  $3p^53d^54d$ . As expected the major contribution to the giant resonance observed in  $\text{Mn}^{2+}$  comes from  $3p \rightarrow 3d$  transitions and to a lesser extent  $3p \rightarrow 4s$  transitions. The higher Rydberg  $3p \rightarrow 5s$  and the  $3p \rightarrow 4d$  transitions are seen to occur with appreciable oscillator strength, while the  $3p \rightarrow 6s$  transition array was found to be negligible.

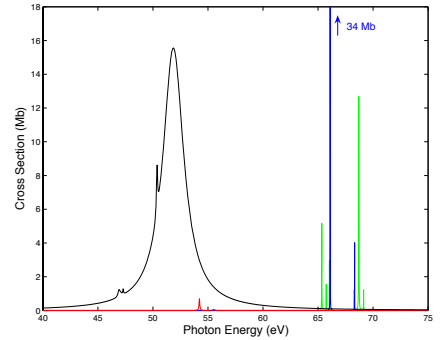


FIG. 2: The calculated cross section  $\sigma$  for each of the following transitions:  $3p \rightarrow 3d$  (black),  $3p \rightarrow 4s$  (red),  $3p \rightarrow 5s$  (blue) and  $3p \rightarrow 4d$  (green).

Fig. 3 shows the calculated (partial) cross sections,  $\sigma_i$ , for a number of low-lying terms of the  $3d^5$  configuration. Where possible the calculated term energies have been shifted to known values [22]. It should be noted that the last of these states are not listed in [22] but are calculated here and in [24]. It is difficult to ascertain which terms contribute most to the overall shape of the photoabsorption spectrum of  $\text{Mn}^{2+}$ .

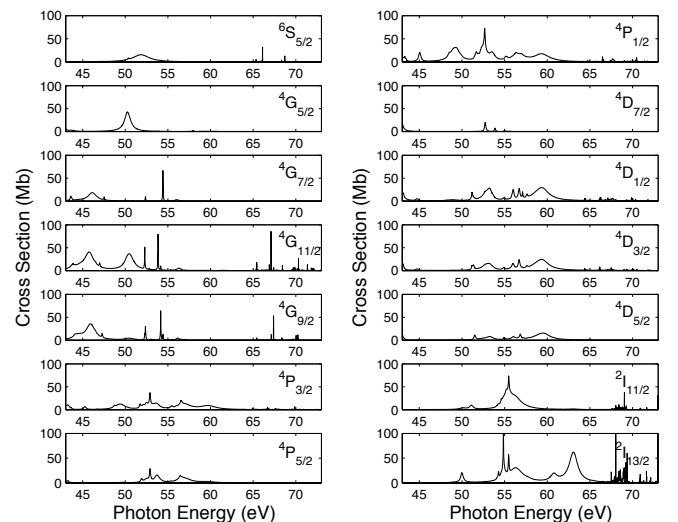


FIG. 3: Calculated cross sections for 3p excitations arising from all levels of the  $3d^5$   ${}^6S$  multiplet,  $3d^5$   ${}^4G$  multiplet,  $3d^5$   ${}^4P$  multiplet,  $3d^5$   ${}^4D$  multiplet and the  $3d^5$   ${}^2I$  multiplet.

Having computed the (partial) cross sections of each of the ground configuration terms, including higher lying terms not shown in Fig. 3, each cross section was weighted by an appropriate Boltzmann factor. The resulting absorption profile for a range of electron temperatures 0.5 – 5.0 eV is presented in Fig 4(a). Also presented in Fig 4(b), for the same range of temperatures, is a comparison between the calculated absorption spectra convolved with a Gaussian instrument function of width 0.07 eV and the experimental photoabsorption spectrum. The theoretical data have been shifted by +0.75 eV to fit the  $3p - 4s$  resonances of the experimental spectrum. Comparing these data with observation, it is seen that the relative contributions expected for a plasma electron temperature ( $T_e$ ) of 2.5 eV fit the experimental data quite well and compare favourably with the temperature quoted for  $\text{Cr}^{2+}$  ( $T_e = 3.3$  eV) [3]. This accounts for the presence of metastables in the plasma which contribute to the photoabsorption spectrum of  $\text{Mn}^{2+}$  recorded here. It is interesting to note that a much cooler plasma ( $T_e = 1.0$  eV) produces a spectrum considerably closer to that predicted by Dolmatov [9], as can be seen from Fig 4(b).

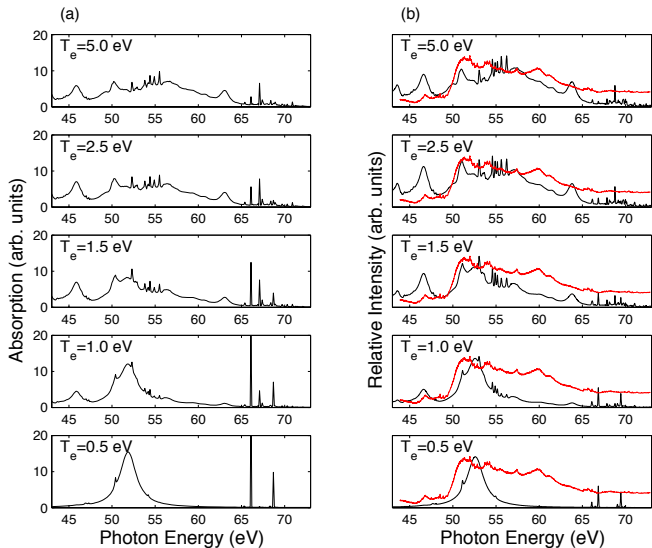


FIG. 4: (a) Synthetic photoabsorption cross section for 3p excitation from the  $\text{Mn}^{2+} 3d^5$  configuration. (b) Comparison of synthetic  $\text{Mn}^{2+}$  spectra (black) with experimental  $\text{Mn}^{2+}$  spectrum (red).

### B. Synthetic spectra for 3p excitations of $\text{Mn}^{3+}$

The ground state of  $\text{Mn}^{3+}$  is  $3d^4 {}^5D$  and the positions of the excited  $3d^4 {}^3P$  triplet (2.560 eV),  $3d^4 {}^3H$  triplet (2.638 eV),  $3d^4 {}^3F$  triplet (2.825 eV) and  $3d^4 {}^3G$  triplet (3.153 eV) have been previously established [25]. Therefore there exists an enormous number of terms close in energy to the ground state that could contribute to the

overall shape of the  $\text{Mn}^{3+}$  ion spectrum in a hot plasma. The basis states listed in Table II were used to perform configuration interaction Hartree-Fock calculations using the HXR mode of the Cowan code [23].

TABLE II: Configurations included in the CI calculation for the 3p-excitations of  $\text{Mn}^{3+}$

Ground states	Discrete states	Continuum channels
$3p^6 3d^4$	$3p^5 3d^5$ <sup>a</sup>	$3p^6 3d^3 4p$ $3p^6 3d^3 + \epsilon l$
$3p^6 3d^3 4s$	$3p^5 3d^4 4s$ <sup>a</sup>	$3p^6 3d^3 5p$ $3p^6 3d^2 4s + \epsilon' l$
	$3p^5 3d^4 5s$ <sup>a</sup>	$3p^6 3d^3 6p$
	$3p^5 3d^4 6s$ <sup>a</sup>	$3p^6 3d^3 4f$
	$3p^5 3d^4 4d$ <sup>a</sup>	$3p^6 3d^3 5f$
	$3p^5 3d^3 4s^2$ <sup>a</sup>	$3p^6 3d^3 6f$

<sup>a</sup> denotes levels from which autoionization was energetically possible.

Autoionization calculations were performed to determine the decay width of the excited  $3p^{-1}$  states. Again the decay schemes were restricted to those denoted in table II, from the excited states labelled 'a' to both continuum channels. Figure 5 shows the calculated cross section for all terms of the following transition arrays:  $3p^6 3d^4 \rightarrow 3p^5 3d^5$ ,  $3p^6 3d^4 4s$ ,  $3p^6 3d^4 5s$ ,  $3p^6 3d^4 6s$ ,  $3p^6 3d^4 4d$ .

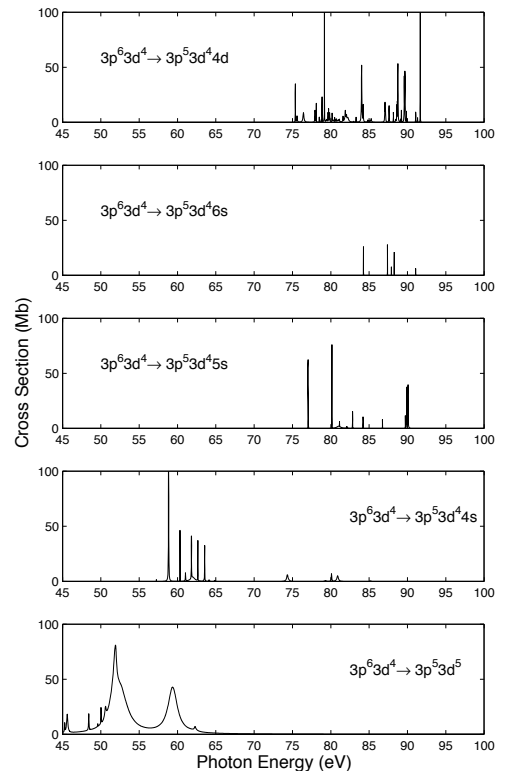


FIG. 5: The calculated cross section  $\sigma$  for each of the following transitions:  $3p \rightarrow 3d$ ,  $3p \rightarrow 4s$ ,  $3p \rightarrow 5s$ ,  $3p \rightarrow 6s$  and  $3p \rightarrow 4d$ .

The  $3p \rightarrow 3d$  transitions contribute most to the giant

resonance observed in  $\text{Mn}^{3+}$  with minor contributions coming from the  $3p \rightarrow 4s$  transitions. The  $3p \rightarrow ns$  ( $n \geq 5$ ) and the  $3p \rightarrow 4d$  transitions occur at higher energies than experimentally recorded here. As was observed in [3] for  $\text{Cr}^{2+}$  (which is isoelectronic with  $\text{Mn}^{3+}$ ), photoabsorption from states of the  $3d^3 4s$  configuration does not play a significant role in determining the overall shape and structure of the experimental photoabsorption spectrum and they are therefore omitted from this figure.

Fig. 6 shows the calculated (partial) cross sections,  $\sigma_i$ , from each of the  $3d^4 \ ^5D, \ ^3P, \ ^3H, \ ^3F$  and  $\ ^3G$  states. Where possible the calculated term energies have been shifted to known values [25]. It is clear that each term contributes to the overall photoabsorption spectrum of  $\text{Mn}^{3+}$ .

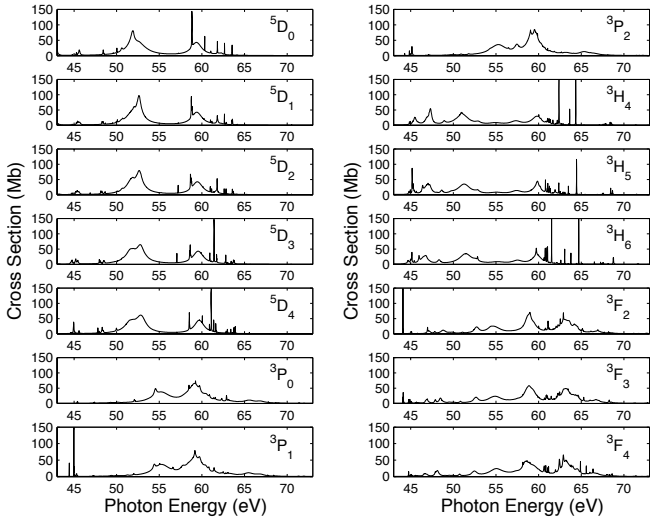


FIG. 6: Calculated cross sections for  $3p$  excitations arising from all levels of the  $3d^4 \ ^5D$  multiplet,  $3d^4 \ ^3P$  multiplet,  $3d^4 \ ^3H$  multiplet,  $3d^4 \ ^3F$  multiplet and the  $3d^4 \ ^3G$  multiplet.

In calculating the synthetic spectra all levels of the  $3d^4$  configuration including those higher than presented in Fig. 6 were considered as they are expected to make a small contribution to the overall spectrum. By assuming thermodynamic equilibrium in the plasma plume, the relative contribution of each term of the ground state ( $3d^4$ ) configuration was determined using a Boltzmann distribution. The resulting absorption profile for a range of electron temperatures 0.5 – 10.0 eV is presented in Fig 7(a). Also presented in Fig 7(b), for the same range of temperatures, is a comparison between the calculated absorption spectra convolved with a Gaussian instrument function of width 0.07 eV and the experimental photoabsorption spectrum. The theoretical data have been shifted by +1.5 eV to fit the lower energy range of the experimental spectrum where the strong broad structure is due to  $3p - 3d$  transitions. The synthetic spectrum produced with a plasma electron temperature of 10.0 eV compares best with the experimental data; the overall

agreement is good in that the main features are reproduced.

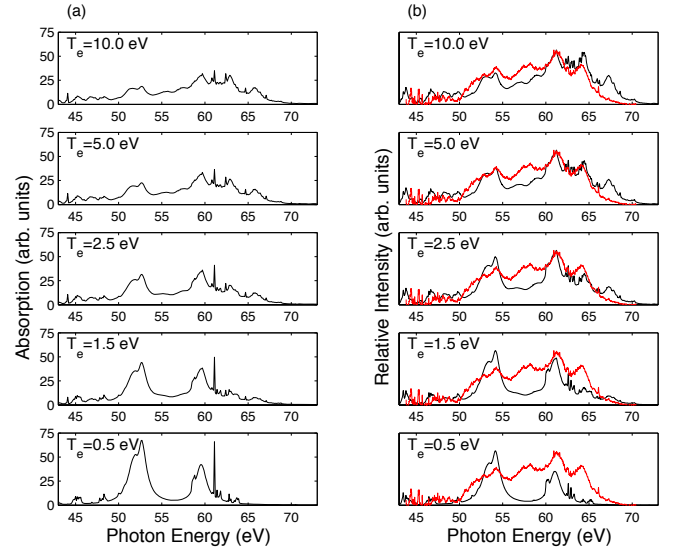


FIG. 7: (a) Synthetic photoabsorption cross section for  $3p$  excitation from the  $\text{Mn}^{3+} \ 3d^4$  configuration. (b) Comparison of synthetic spectra (black) with experimental spectrum (red).

#### IV. CONCLUSION

Photoabsorption spectra of a manganese plasma recorded using the dual laser plasma technique have been presented. The  $\text{Mn}^{2+}$  and  $\text{Mn}^{3+}$  ions were isolated and recorded at a time delay of 80 ns and 30 ns respectively and at a position of 1.00 mm from the optic axis. The 43 – 73 eV photon energy range was found to be dominated by the  $3p$ - $3d$  giant resonances and to a lesser extent the  $3p$ - $4s$  resonances in both spectra. Synthetic  $\text{Mn}^{2+}$  and  $\text{Mn}^{3+}$  spectra were calculated using the Hartree-Fock method while accounting for absorption from excited states of the ground configuration weighted by an appropriate Boltzmann factor. For  $\text{Mn}^{2+}$  a plasma temperature of 2.5 eV was found to be suitable while a plasma temperature of 10.0 eV gave best agreement for  $\text{Mn}^{3+}$ . In this way metastable contributions to the recorded spectra have been accounted for.

#### Acknowledgments

This work was supported by the Irish Government National Development Plan including the Basic Research Grants Scheme of the Irish Research Council for Science Engineering and Technology / Science Foundation Ireland and also the Higher Education Authority Programme for Research in Third Level Institutions.

- 
- [1] J. T. Costello, E. T. Kennedy, B. F. Sonntag, and C. W. Clark, *Phys. Rev. A* **43**, 1441 (1991).
- [2] C. McGuinness, M. Martins, P. Wernet, B. F. Sonntag, P. van Kampen, J.-P. Mosnier, E. T. Kennedy, and J. T. Costello, *J. Phys. B* **32**, L583 (1999).
- [3] C. McGuinness, M. Martins, P. van Kampen, J. Hirsch, E. T. Kennedy, J.-P. Mosnier, W. W. Whitty, and J. T. Costello, *J. Phys. B* **33**, 5077 (2000).
- [4] J. B. West, J. E. Hansen, B. Kristensen, F. Folkmann, and H. Kjeldsen, *J. Phys. B* **36**, L327 (2003).
- [5] J. W. Cooper, C. W. Clark, C. L. Cromer, T. B. Lucatorto, B. F. Sonntag, E. T. Kennedy, and J. T. Costello, *Phys. Rev. A* **39**, 6074 (1989).
- [6] H. Kjeldsen, F. Folkmann, B. Kristensen, J. B. West, and J. E. Hansen, *J. Phys. B* **37**, 1321 (2004).
- [7] H. Kjeldsen, B. Kristensen, F. Folkmann, and T. Andersen, *J. Phys. B* **35**, 3655 (2002).
- [8] V. K. Dolmatov, *J. Phys. B* **26**, L79 (1993).
- [9] V. K. Dolmatov, *J. Phys. B* **29**, L687 (1996).
- [10] V. K. Dolmatov, *J. Phys. B* **29**, L673 (1996).
- [11] J. P. Connerade and V. K. Dolmatov, *J. Phys. B* **29**, L831 (1996).
- [12] V. K. Dolmatov, *J. Phys. B* **31**, 999 (1998).
- [13] D. Donnelly, K. L. Bell, and A. Hibbert, *Phys. Rev. A* **54**, 974 (1996).
- [14] D. Donnelly, K. L. Bell, and A. Hibbert, *J. Phys. B* **29**, L693 (1996).
- [15] D. Donnelly, K. L. Bell, and A. Hibbert, *J. Phys. B* **30**, L285 (1997).
- [16] D. Donnelly, K. L. Bell, and A. Hibbert, *J. Phys. B* **31**, L971 (1998).
- [17] D. Kilbane, E. T. Kennedy, J.-P. Mosnier, P. van Kampen, and J. T. Costello, *J. Phys. B* **38**, L1 (2005).
- [18] R. J. Radwanski and Z. Ropka, *Journal of Magnetism and Magnetic Materials* **272-276**, e259 (2004).
- [19] M. J. D. Coey, M. Viret, L. Ranno, and K. Ounadjela, *Phys. Rev. Lett.* **75**, 3910 (1995).
- [20] Y.-S. Su, T. A. Kaplan, and S. D. Mahanti, *Phys. Rev. B* **61**, 1324 (2000).
- [21] E. T. Kennedy, J. T. Costello, J.-P. Mosnier, A. A. Cafolla, M. Collins, L. Kiernan, U. Köble, M. H. Sayyad, M. Shaw, and B. F. Sonntag, *Opt. Eng.* **33**, 3984 (1994).
- [22] C. E. Moore, *Atomic Energy Levels vol II* (Circular of the National Bureau of Standards 467, 1958).
- [23] R. D. Cowan, *The Theory of Atomic Structure and Spectra* (University of California Press, Berkeley, CA, 1981).
- [24] A. Pasternak and Z. B. Goldschmidt, *Phys. Rev. A* **9**, 1022 (1974).
- [25] I. S. Bowen, *Phys. Rev.* **52**, 1153 (1937).